

ANALYZING TERRASAR-X AND COSMO-SKYMED HIGH-RESOLUTION SAR DATA OF URBAN AREAS

Mingsheng Liao*, Timo Balz, Lu Zhang, Yuanyuan Pei, Houjun Jiang

State Key Laboratory of Information Engineering in Surveying, Mapping and Remote Sensing,
Wuhan University, 129 Luoyu Road, Wuhan, China
liao@whu.edu.cn

KEY WORDS: SAR, high-resolution, urban area, InSAR, Persistent Scatterer Interferometry

ABSTRACT:

The new high-resolution synthetic aperture radar (SAR) satellite systems offer new possibilities for urban remote sensing. COSMO-SkyMed and TerraSAR-X operate in X-band and both can deliver data with a spatial resolution of up to one meter. High-resolution SAR data is particularly useful for post-disaster damage assessment and monitoring, because SAR systems operate (almost) weather independent. Interferometric SAR (InSAR) can be used to generate precise 3D models of urban areas, and using Persistent Scatterer Interferometry (PS-InSAR) urban subsidence can be measured precisely.

1. INTRODUCTION

Comparable to the tremendous improvements in the remote sensing sciences caused by the successful launch of IKONOS in 1999, the radar remote sensing sciences will benefit from the new commercial high-resolution spaceborne synthetic aperture radar (SAR) satellite systems. COSMO-SkyMed (De Luca *et al.* 2007), Radarsat-2 (Thompson *et al.* 2008), and TerraSAR-X (Eineder *et al.* 2005) provide spaceborne SAR data in spatial resolutions not available before. With resolutions of up to one meter, the data can be used for urban remote sensing.

SAR has several disadvantages in urban areas, which are related to the wavelength and oblique viewing geometry of SAR systems. In section 2, we describe the problems of SAR remote sensing in urban areas.

But, SAR also has some unique advantages. One advantage is the ability to acquire data under almost all weather conditions, at day and night. SAR systems are active systems, i.e. they transmit and receive their own energy. Therefore, they are independent of the sun. The transmitted microwaves can penetrate clouds; hence, SAR systems can acquire data even during bad weather conditions. Extreme weather conditions, like for example very heavy rainfall, can influence and even hinder the data acquisition though. This happens rather seldom though.

This unique advantage of SAR systems is extremely important in time-critical applications. After the Wenchuan Earthquake (Parsons *et al.* 2008) on May 12, 2008, heavy rainfall hindered the use of optical remote sensing systems in the affected area. SAR was for some regions the only available spaceborne data source in the days following the earthquake. SAR is widely used for post-seismic damage assessment (Shinozuka *et al.* 2000; Yonezawa and Takeuchi 2001; Matsuoka and Yamazaki 2005; Stramondo *et al.* 2006; Gamba *et al.* 2007; Chini *et al.* 2008). Typically pre-disaster data is compared with post-disaster data, but this was not possible after the Wenchuan Earthquake, because almost no pre-disaster high-resolution SAR data was available. Nevertheless, TerraSAR-X and COSMO-SkyMed delivered important data for the disaster

management (Balz *et al.* 2008). High-resolution SAR was, for example, widely used to monitor (Shao *et al.* 2008) the so-called quake lakes (Stone 2008). High-resolution SAR can also be used for damage assessment in urban areas (Balz and Liao 2009), which will be demonstrated in section 3.

The weather independence is not the only advantage of SAR systems. SAR systems can precisely measure distances. Using two receiving antennas and a technique called interferometric SAR (InSAR) digital elevation models (DEM) can be generated. Instead of using two antennas at the same time, which is called single-pass InSAR, the same sensor can acquire data twice at different times, which is called multi-pass InSAR. This technique is used by today's satellites. In this way, they are able to acquire precise height models, which will be shown in section 4. Using interferometric SAR data acquired over a long time, persistent scatterers (PS) can be determined and observed. This allows for even more precise measurements of height differences. This technique is called Persistent Scatterer Interferometry (PS-InSAR) (Ferretti *et al.* 2000, 2001) and can be used for subsidence measurement (Hilley *et al.* 2004). Typically, this requires a huge amount of data. Using small stack PS-InSAR, subsidence can be measured with less data. This is described in section 5. Finally, conclusions will be drawn.

2. HIGH-RESOLUTION SAR DATA OF URBAN AREAS

SAR systems acquire images from an oblique viewing geometry. The geometry differs in azimuth direction, which is the heading direction of the sensor platform, and range direction, which is the direction of the radar signal and is normally perpendicular to azimuth.

In azimuth, the geometry depends on the Doppler Effect. For non-moving objects, a SAR system can reach very high resolutions in azimuth. In range direction the position of an object is determined by the runtime of the signal, which directly correlates to the length of the signal path. This leads to several typical SAR effects, which only occur in range direction.

* Corresponding author.

The first effect, the so-called layover, is visible in Figure 1. Figure 1 shows the Mingsheng Bank building in Wuhan, China. The building is 331.3 m height and is the tallest building in Wuhan. It was the 18th tallest building in the world when it was finished in 2007. The image was acquired as part of the Wuhan University TerraSAR-X test site, a joint project between the Wuhan University, Beijing Spot Image and Infoterra, to promote the use of high-resolution SAR images.

The image in Figure 1 was taken from an ascending orbit and was illuminated from the left side. The building can clearly be recognized. Strong reflections occur on the edge of the building and at the rooftop. The corner-reflection at the foot point is clearly identifiable. The top of the building can be seen far on the left side of Figure 1, whereas the bottom is in the center of Figure 1. This is the so-called layover. Because the top of the building is closer to the sensor and because the position of an object in range depends on signal's time of flight, the building's roof is mapped closer to the sensor than the bottom.

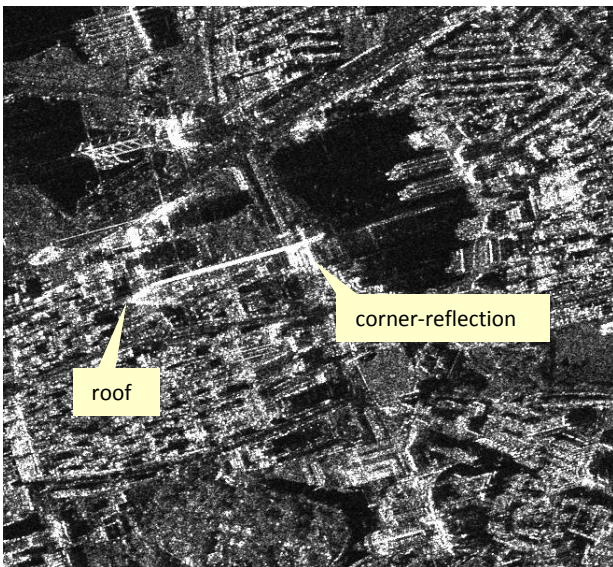


Figure 1. TerraSAR-X spotlight image from October 31, 2008, acquired in VV polarization from an ascending orbit.

Another effect caused by the oblique viewing geometry is the radar shadow. The dark area in the center of the image is no shadow though, it is a small lake. Calm water acts like a mirror in X-band SAR images, therefore the energy transmitted by the SAR sensor is forward scattered by the lake and is not backscattered to the sensor; hence, lakes appear dark in SAR images.

Figure 2 shows the same area as Figure 1, but the image was acquired from a descending orbit. The image is therefore illuminated from the right side.

The double-bounce at the descending image (Figure 2) is very strong and the side-lobes of this extreme reflection can be seen throughout the whole scene. Double-bouncing occurs when microwaves are forward scattered by a smooth surface, for example a lake, hit another surface, for example a building, and are scattered back to the sensor.

The radar cross section (RCS) for the double bounce scattering from a building can be approximated using the physical optics approximation (Dong *et al.* 1997):

$$\sigma_{db} \approx \frac{16\pi}{\lambda^2} R_{p1}^2 \cdot R_{p2}^2 \cdot A^2 \cdot \sin^2 \theta_i \cdot \cos^8 \phi \left[\frac{\sin(k_0 \cdot L \cdot \sin \theta \cdot \sin \phi)}{k_0 \cdot L \cdot \sin \theta \cdot \sin \phi} \right]$$

where R_{p1} and R_{p2} are the Fresnel Reflection Coefficient of the wall and the ground respectively. θ_i is the incidence angle, k_0 is the wave number, L is the length of the flat rectangular plate (see Dong *et al.* 1997), A is the area of the wall, and ϕ is the aspect angle. The aspect angle is the orientation of the building relating to the looking direction of the sensor with $\phi = 0^\circ$ if the wall is perpendicular to the looking direction.

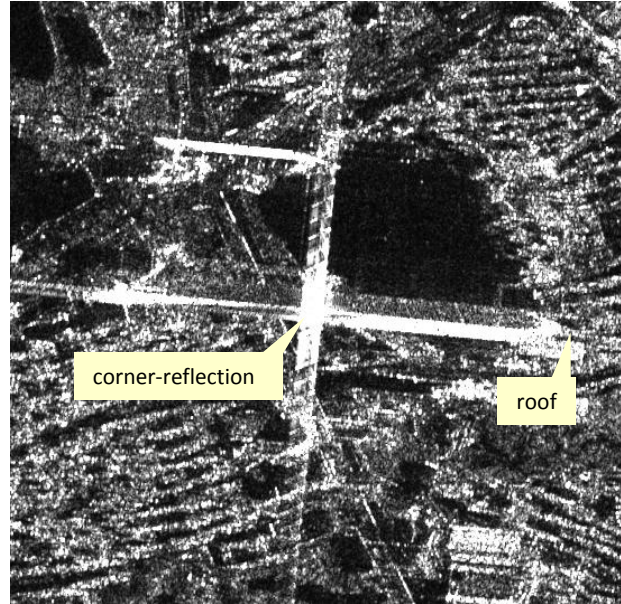


Figure 2. TerraSAR-X spotlight image from October 18, 2008, acquired in VV polarization from a descending orbit.

The extreme double-bounce reflection of the Mingsheng Bank building is therefore related to the extreme height of the building, because σ_{db} shows a quadratic dependence with the wall area, and due to the very small aspect angle ϕ . Additionally, the small lake in front of the building strongly reflects the incoming energy from the radar with a high Fresnel Reflection Coefficient, amplifying the extreme backscattering. Due to the lake in near-range, even triple-bounce reflections can be observed. Triple-bouncing is not very common in SAR images of urban areas. But, triple-bouncing frequently occurs at bridges over water (Lee *et al.* 2006).

3. HIGH-RESOLUTION SAR FOR POST-DISASTER DAMAGE ASSESSMENT IN URBAN AREAS

The new high-resolution SAR satellite systems have been used for damage assessment and post-disaster risk monitoring after the Wenchuan Earthquake from May 12, 2008. High-resolution SAR is a reliable data source, because of its all-weather imaging capabilities. In disaster management, this is a crucial point. But, SAR data is difficult to interpret. Because of the oblique viewing geometry of SAR, ambiguities and occlusions hinder the SAR image interpretation, especially in urban and mountainous areas.

In Figure 3, a TerraSAR-X image of Beichuan can be seen. Beichuan was severely damaged by the Wenchuan Earthquake and by earthquake induced landslides. Beichuan is located in a deep valley, a difficult terrain for radar remote sensing.

The SAR image shown in Figure 3 was taken from a descending orbit; hence, the sensor was looking from the right side. The landslides on the western sides of the mountains, like for example the so-called New-Middle-School Landslide, can be identified in this SAR image.

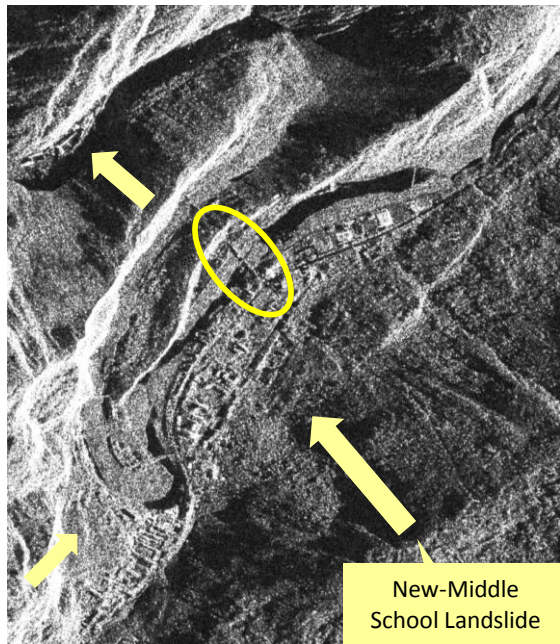


Figure 3. TerraSAR-X stripmap image of Beichuan acquired from a descending orbit on May 15, 2008.

But, due to fore-shortening and layover, the landslides on the eastern sides cannot be identified. For this purpose, a second SAR image, taken from an ascending orbit, is needed. Figure 4 shows a TerraSAR-X image of Beichuan acquired from an ascending orbit, two days after the image shown in Figure 3 was taken. In Figure 4, the landslides on the western sides are not identifiable.

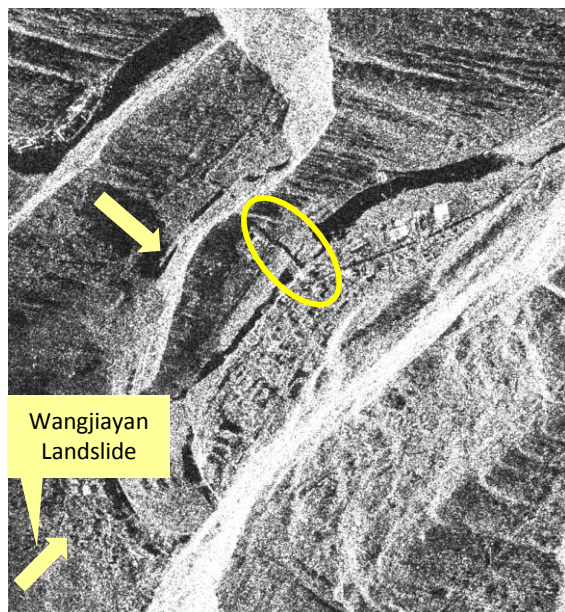


Figure 4. TerraSAR-X stripmap image of Beichuan acquired from an ascending orbit on May 17, 2008.

Ascending-descending image pairs are therefore recommended for SAR image interpretation in urban and mountainous areas. But using ascending-descending image pairs reduces the temporal resolution. To improve the temporal resolution, different sensor systems should be used together. Useful combinations do not only include ascending-descending image pairs, but also combinations of imaging modes with different resolutions. The COSMO-SkyMed image from Beichuan shown in Figure 5 was acquired in spotlight mode. The image has a spatial resolution of one meter. The stripmap images shown in Figure 3 and Figure 4 have a spatial resolution of three meters.

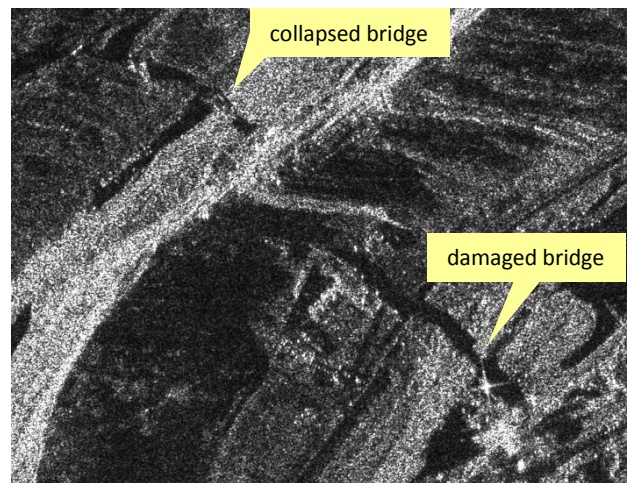


Figure 5. COSMO-SkyMed spotlight image acquired from an ascending orbit on May 14, 2008.

Figure 5 shows two bridges in Beichuan, which are marked with an ellipse in Figure 3 and Figure 4. The status of the bridges cannot be determined in the stripmap images, but the spatial resolution of the spotlight image is high enough to identify the damages. The western bridge collapsed, whereas the eastern bridge is only damaged, which can be seen in the shadow casted by the bridge.

In Figure 6, three SAR images of Dujiangyan city can be seen. Dujiangyan is located near the Zipingpu dam (Kerr and Stone 2009). Figure 6(a) shows a COSMO-SkyMed image acquired from a descending orbit on May 13, 2008, one day after the quake. It was the first high-resolution SAR image from the area. The high and chaotic reflections of the buildings near the street are indicators for possible building damages (Balz and Liao 2009). The COSMO-SkyMed image has strong sidelobes all over the image, disturbing the interpretations.

Figure 6(b) shows a Terra-SAR-X spotlight image taken on May 15, 2008, from a descending orbit. The spatial resolution is higher and the image has much less sidelobes. The buildings near the street also have strong and chaotic backscatter. In Figure 6(c), a TerraSAR-X stripmap image acquired on May 22, 2008, from an ascending orbit can be seen. No strong reflections are visible and the buildings near the street seem undamaged on the first glance. But, although the shadow is almost linear, the layover seems chaotic, which is also indicating severe building damage.

The TerraSAR-X images seem clearer and they suffer less from sidelobes in the Dujiangyan scenes. But, as can be seen in Figure 6, the differences are rather small. Differences caused by different looking angles, image modes, and orbits are more significant.

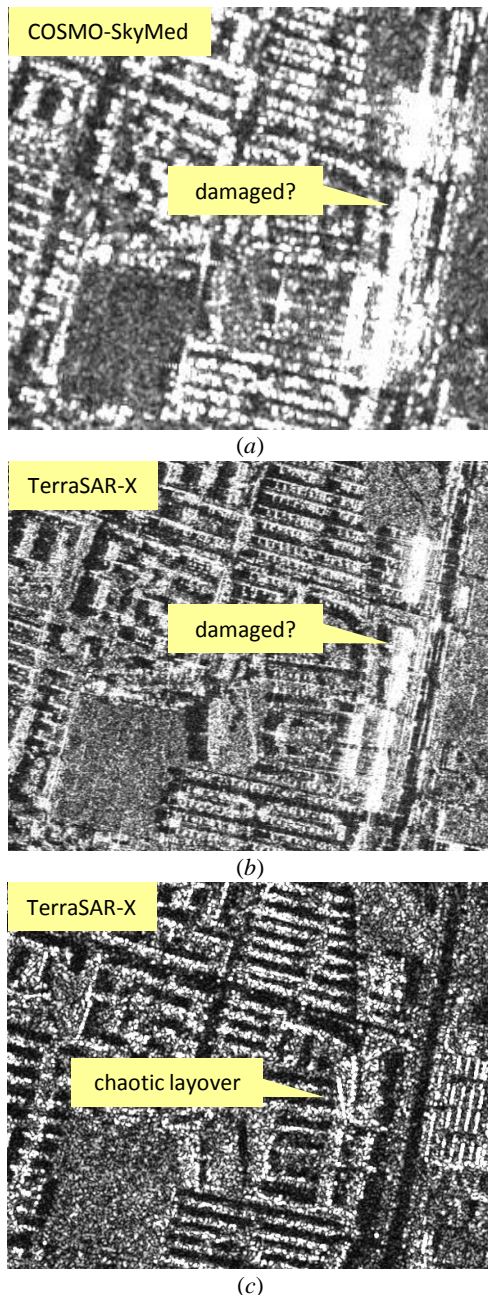


Figure 6. Descending COSMO-SkyMed image (a), descending TerraSAR-X image (b), and ascending TerraSAR-X image (c) of Dujiangyan city.

4. TERRASAR-X INSAR DATA OF SHANGHAI

To evaluate the interferometric performance of TerraSAR-X, we use a pair of TerraSAR-X SLC data over Shanghai. Shanghai is, with over 20 million inhabitants, the largest city in China in terms of population. The city is located at the Yangtze River Delta. The city area is rather flat. Shanghai is bisected by the Huangpu River.

Since the 1990s, the economical reforms lead to a remarkable development of the city, making it one of the world's financial centers and the world's biggest cargo port.

The two TerraSAR-X images were acquired in stripmap mode from descending orbits on April 21 and August 20, 2008. They cover the urban and most suburban areas of Shanghai. Figure 7(a) shows the TerraSAR-X test scene.

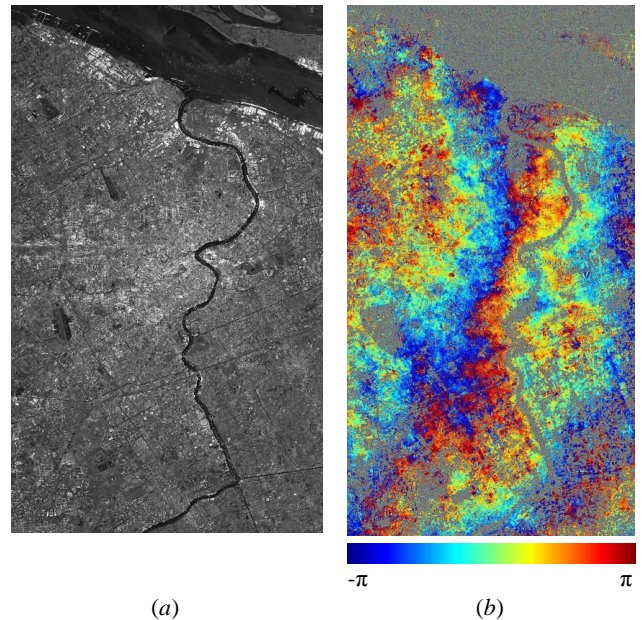


Figure 7. TerraSAR-X InSAR results over Shanghai. Amplitude image (a); Interferometric phase (b).

The urban area and dock area show as bright features, due to high backscattering, while water bodies (sea and river), as well as, for example, the runways on the airport show dark tones, as a result of very low backscattering. The suburban areas appear in medium gray levels. Figure 8 shows the interferometric phase over the Pudong area in Shanghai. Figure 9 shows the coherence in the same area. The high-rise buildings forming the Pudong skyline can be identified clearly in the interferometric phase image.

The perpendicular baseline is about 61.4 m, which is moderate for X-band SAR systems. Therefore, good coherence, as high as 0.8, can be maintained in most urban areas, even with a long temporal baseline of 121 days. Meanwhile, coherence is nearly lost in most suburban or rural areas, which is likely due to surface changes between the two acquisitions in spring and summer respectively.

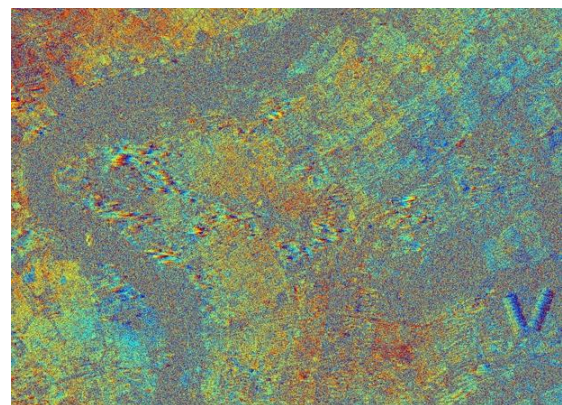


Figure 8. Interferometric phases over the Pudong area in Shanghai.

Although from a single interferometric experiment we cannot derive any information of surface deformations, it does reveal that TerraSAR-X data is suitable for SAR interferometric studies over urban areas, even with a long temporal baseline. Furthermore, it is expected that PS-InSAR with time series of TerraSAR-X data can be successfully applied to subsidence monitoring in urban areas such as Shanghai.



Figure 9. Coherence image of the Pudong area in Shanghai.

5. SMALL STACK PS-INSAR OVER SHANGHAI

Since the 1920s, Shanghai is suffering from subsidence. This has gotten worse with the increasing urban development since the 1990s

Differential interferometry (D-InSAR) has been widely applied for large-area subsidence monitoring. However, this technique is difficult to employ for long-term monitoring, due to temporal decorrelation, atmospheric effects, and other limitations. In order to overcome the major problems of D-InSAR, the Persistent Scatterer Interferometry (PS-InSAR) has been developed. Using PS-InSAR, the subsidence can be precisely measured.

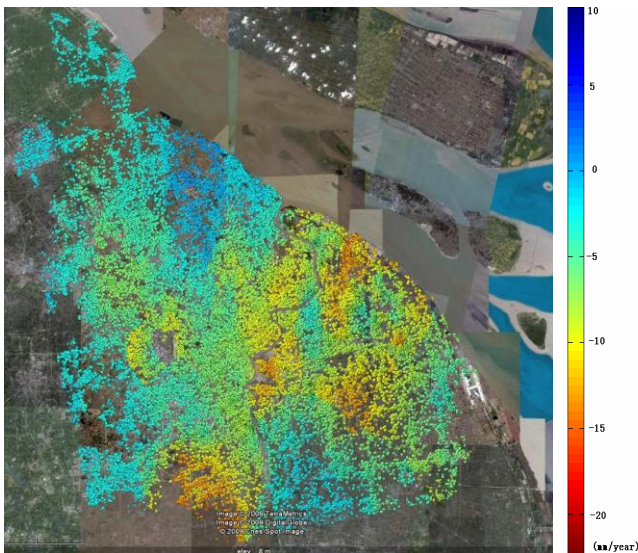


Figure 10. Subsidence measured over Shanghai using PS-InSAR.

For the Shanghai study area, eight ENVISAT ASAR IMS images (Track 497, Frame 621), acquired from October 2007 to October 2008, are combined to generate the differential interferograms. The perpendicular baselines range from -325 m to 254 m. The maximum difference in the Doppler Centroid frequency is about 7.2 Hz. The processed area is approximately 5000 km². The SRTM C-Band DEM is used for the topographic phase removal. 16 differential interferograms were generated. In total 821,477 PS points are extracted from the short-time InSAR stack (Lu *et al.* 2008). Using the spatio-temporal unwrapping method, we can obtain the annual average subsidence rate. We found the subsidence rate to be in the range of -25 to 10 mm/year. Figure 10 shows the subsidence map obtained by short-term stack PS-InSAR. It shows a good consistency with

the reference subsidence map derived from leveling measurements in that the main subsidence areas coincide well with each other.

We plan to test small stack PS-InSAR using high-resolution SAR over Shanghai, soon. The necessary data is acquired at the moment. High-resolution PS-InSAR is a promising technique. Adam *et al.* (2008) show that while using PS-InSAR with high-resolution SAR images, many persistent scatterers can be found in one building. By grouping neighbored persistent scatterers, combined movement estimation can be set up and specific displacement models for the group movement can be employed (Gernhardt and Hinz 2008).

6. CONCLUSIONS

Spaceborne high-resolution SAR images are a new, reliable, and weather independent data source. With spatial resolutions up to one meter, remote sensing applications in urban areas are possible. SAR image interpretation is rather difficult though. Because of the oblique viewing geometry, occlusions and ambiguities frequently occur in SAR images. SAR images of urban areas are especially difficult to interpret. Layover and shadows of high-rise buildings disturb the image. The artificial structures forward scatter a great amount of the energy transmitted by the SAR system. Double- and multi-bounces frequently occur in SAR images of urban areas, further disturbing the interpretation. SAR images are important data sources for time-critical operations in need of weather independent surveillance. Disaster management benefits strongly from high-resolution SAR. For example, after the Wenchuan Earthquake, SAR was widely used for post-disaster surveillance.

For time-critical missions, the temporal resolution of a system is crucial. The modern high-resolution SAR satellites have a high revisiting frequency. The repeat-orbit period of TerraSAR-X is only 11 days, compared with 35 days for ERS or Envisat ASAR and 24 days for Radarsat-1. COSMO-SkyMed's four satellite constellation has an even higher repetition rate. The combined use of various data sources can further increase the temporal resolution. Using data from different sensors is always difficult, even if the sensors operate with almost similar characteristics. For manual interpretation, COSMO-SkyMed and TerraSAR-X data can be combined. A combined use of the data for automated procedures is more difficult, but seems possible for the real parts of the SAR images.

Another important feature of SAR systems is their precise measurement of distances, which can be used for the creation of DEMs using InSAR. High-resolution InSAR allows the creation of precise height models of urban areas. Using high-resolution persistent scatterer interferometry differences in the subsidence of single buildings can be identified.

We are just about to discover the whole range of new possibilities and applications provided by the new high-resolution SAR systems. There are new applications for the weather independent high-precision measurements of high-resolution SAR systems and it is time to discover them.

ACKNOWLEDGMENT

The authors would like to thank the Infoterra GmbH, Beijing Spot Image, and Beijing Earth Observation Inc. This work was supported by the National Key Basic Research and Development Program of China (Contract No. 2007CB714405), National 863 Program of China (Contract No. 2007AA12Z180), and China Postdoctoral Science Foundation (20080440952).

REFERENCES

- Adam, N., Eineder, M., Yague-Martinez, N. and Bamler, R., 2008. High-resolution interferometric stacking with TerraSAR-X. In: *Proc. International Geoscience and Remote Sensing Symposium (IGARSS 2008)*, Boston, USA.
- Balz, T., Scheuchl, B. and Li, D.R., 2009. Sichuan Earthquake (1): suitability of satellite images in rapid response. *GIM International*, 22 (10), pp. 13-15.
- Balz, T. and Liao, M.S., 2009. Building damage detection using post-seismic high-resolution SAR satellite data. *International Journal of Remote Sensing*, in press.
- Chini, M., Bignami, C., Stramondo, S. and Pierdicca, N., 2008. Uplift and subsidence due to the 26 December 2004 Indonesian earthquake detected by SAR data. *International Journal of Remote Sensing*, 29, pp. 3891-3910.
- De Luca, G.F., Marano, G., Piemontese, M., Versini, B., Caltagirone, F., Casonato, G., Coletta, A. and De Carlo, M., 2007. Interoperability, expandability and multi mission-sensor COSMO-SkyMed capabilities. In: *Proc. International Geoscience and Remote Sensing Symposium (IGARSS 2007)*, Barcelona, Spain.
- Dong, Y., Forster, B. and Ticehurst, C., 1997. Radar backscatter analysis for urban environments. *International Journal of Remote Sensing*, 18, pp. 1351-1364.
- Eineder, M., Breit, H., Fritz, T., Schuettler, B. and Roth, A., 2005. TerraSAR-X SAR products and processing algorithms. In: *Proc. International Geoscience and Remote Sensing Symposium (IGARSS 2005)*, Seoul, Korea.
- Ferretti, A., Prati, C. and Rocca, F., 2000. Nonlinear subsidence rate estimation using permanent scatterers in differential SAR interferometry. *IEEE Transactions on Geoscience and Remote Sensing*, 38, pp. 2202-2212.
- Ferretti, A., Prati, C. and Rocca, F., 2001. Permanent scatterers in SAR interferometry. *IEEE Transactions on Geoscience and Remote Sensing*, 39, pp. 8-20.
- Gamba, P., Dell'Acqua, F. and Trianni, G., 2007. Rapid damage detection in the Bam area using multitemporal SAR and exploiting ancillary Data. *IEEE Transactions on Geoscience and Remote Sensing*, 45, pp. 1582-1589.
- Gernhardt, S. and Hinz, S., 2008. Advanced displacement estimation for PSI using high resolution SAR Data. In: *Proc. International Geoscience and Remote Sensing Symposium (IGARSS 2008)*, Boston, USA.
- Hilley, G.E., Buergermann, R., Ferretti, A., Novali, F. and Rocca, F., 2004. Dynamics of slow-moving landslides from permanent scatterer analysis. *Science*, 304, pp. 1952-1955.
- Kerr, R.A. and Stone, R., 2009. A human trigger for the Great Quake of Sichuan? *Science*, 323, p. 322.
- Lee, J.S., Ainsworth, T.L., Krogagor, E. and Boerner, W.-M., 2006. Polarimetric analysis of radar signature of a man-made structure. In: *Proc. International Geoscience and Remote Sensing Symposium (IGARSS 2006)*, Denver, Colorado.
- Lu, L.J., Liao, M.S., Wang, C.C., Tian, X., Li, D.R., Fang, Z., Wang, H.M., Yang, L.J., Fang, Z.L., 2008. A new method of identification of stable pointwise target in small SAR dataset. In: *Proc. 2008 Dragon Symposium, ESA SP-655*, Beijing, China.
- Matsuoka, M. and Yamazaki, F., 2005. Building damage mapping of the 2003 Bam, Iran, Earthquake using Envisat/ASAR intensity imagery. *Earthquake Spectra*, 21, pp. S285-S294.
- Parsons, T., Ji, C. and Kirby, E., 2008. Stress changes from the 2008 Wenchuan Earthquake and increased hazard in the Sichuan basin. *Nature*, 454, pp. 509-510.
- Shao, Y., Gong, H.Z., Wang, S.A., Zhang, F.L. and Tian, W., 2008. Multi-source SAR remote sensing data for rapid response to Wenchuan Earthquake damage assessment [in Chinese]. *Journal of Remote Sensing*, 12, pp. 865-870.
- Shinozuka, M., Ghanem, R., Houshmand, B. and Mansouri, B., 2000. Damage detection in urban areas by SAR imagery. *Journal of Engineering Mechanics*, 126, pp. 779-777.
- Stone, R., 2008. Landslides, flooding pose threats as experts survey quake's impact. *Science*, 320, pp. 996-997.
- Stramondo, S., Bignami, C., Chini, N., Pierdicca, N. and Tertulliani, A., 2006. Satellite radar and optical remote sensing for earthquake damage detection: results from different case studies. *International Journal of Remote Sensing*, 27, pp. 4433-4447.
- Thompson, A.A., Luscombe, A., James, K., and Fox, P., 2008. RADARSAT-2 mission status: capabilities demonstrated and image quality achieved. In: *Proc. 7th European Conference on SAR (EUSAR 2008)*, Friedrichshafen, Germany.
- Yonezawa, H.A. and Takeuchi, S., 2001. Decorrelation of SAR data by urban damage caused by the 1995 Hoyooken-Nanbu earthquake. *International Journal of Remote Sensing*, 22, pp. 1585-1600.